Stochastic and Deterministic Vibration Analysis on Drill-String With Finite Element Method

Conference Paper · November 2013

DOI: 10.1115/IMECE2013-62563

CITATIONS
2

READS
123

2 authors:

Hongyuan Qiu
Memorial University of Newfoundland
9 PUBLICATIONS **33** CITATIONS
SEE PROFILE

James Yang
Memorial University of Newfoundland
46 PUBLICATIONS **168** CITATIONS
SEE PROFILE

Proceedings of the ASME 2013 International Mechanical Engineering Congress & Exposition
IMECE2013
November 15-21, 2013, San Diego, California, USA

IMECE2013-62563

STOCHASTIC AND DETERMINISTIC VIBRATION ANALYSIS ON DRILL-STRING WITH FINITE ELEMENT METHOD

Hongyuan Qiu*
Faculty of Mechanical Engineering and Applied Science
Memorial University of Newfoundland
St John's, Newfoundland, Canada, A1B 3X5
Email:hq1622@mun.ca

Jianming Yang
Faculty of Engineering and Applied Science
Memorial University of Newfoundland
St John's, Newfoundland, Canada, A1B 3X5
Email:jyang@mun.ca

ABSTRACT

Using Euler-Bernoulli beam theory, a finite element model with six degrees of freedom per node is developed for a drill-string assembly. The drill-string is driven by a DC motor on the top and is subjected to distributed loads due to its own weight as well as bit/formation interaction. The model is axial-torsional, lateral-torsional coupled. Under deterministic excitations, the model captures stick-slip behavior in drilling operation. Analysis on its negative effect on drilling performance are made, and potential mitigation measures are also discussed. In random model, the excitations to the drill-bit are modeled as combination of deterministic and random components. Monte Carlo (MC) simulation is employed to obtain the statistics of the response. Two cases of random excitation with different intensities are investigated. The results from MC simulation are compared against that from deterministic case.

Keywords: finite element model, drill-string, nonlinearity, random

NOMENCLATURE

l_e Finite element length
$g = 9.84\ m/s^2$ Gravity Acceleration
$G = 7.6923\times10^{10}\ N/m^2$ Drill-string shear modulus
$E = 210\ Gpa$ Drill-string elastic modulus
$\rho = 7850\ kg/m^3$ Drill-sting density
$E_0 = 4\times10^{10}\ N/m^2$ Rock elastic modulus
$\nu = 0.25$ Poisson ratio
$G_0 = 1.6\times10^{10}\ N/m^2$ Rock shear modulus
$r_0 = 0.2$ Foundation diameter
$\rho_0 = 2100\ kg/m^3$ Rock density
$k_c = 4.27\times10^9\ N/m$ Rock stiffness
$c = 1.05\times10^6$ Rock damping coefficient
$m = 500\ kg$ Stabilizer mass
$k_{st} = 10\ MN/m$ Stabilizer stiffness
$r = 0.03\ m$ Eccentric distance of stabilizer mass
w Average bit speed
$r_b = 0.22$ Bit radius
$L = 0.005\ H$ Motor inductance
$R_m = 0.01\ \Omega$ Armature resistance
$K_m = 6\ V/s$ Motor inductance
$n = 7.2$ Gear ratio of the gearbox
$\alpha = 0.01$
$\beta = 0.01$
$c_1 = 1.35\times10^{-8}$
$c_2 = -1.9\times10^{-4}$
$\xi_0 = 1$
$\alpha_1 = 2$
$\alpha_2 = 1$
$\nu = 0.01$

INTRODUCTION

Drill-strings are slender structures used to dig into the rock in search of oil and gas. Failures of drill-strings are time and money consuming and therefore the dynamics of drill-strings

*Address all correspondence to this author.

must be investigated and carefully controlled. However, the deeper the drill-string reaches underground, the more complex the dynamics will be, and the harder to control. It is well known that downhole vibrations are prevalent causes of drill-string failures. Three primary categories of vibratory loads apply to rotary oil-well downhole equipment: axial, torsional and lateral. It is found that these three vibration mechanisms usually occur simultaneously while drilling. One of the axial vibration forms is bit bounce, which is likely to happen when drilling with roller cone (RC) bits. Severe bit-bounce leads to premature bit and bottom hole assemble (BHA) failure and rate of penetration (ROP) reduction. Sometimes, increasing weight on bit (WOB) and adjusting rotation per minute (RPM) can relieve the problem. For torsional vibration, the most common phenomenon is stick-slip. Stick-slip happens when the rotation of the drill-string is slowed down (or even stopped) and then suddenly increased when the torque overcomes the anti-torque result from the rock cutting and friction. Stick-slip vibration can largely decrease ROP and cause fatigue failure of the drill-bit. Increasing RPM can relieve stick-slip once it is detected. Lateral vibration is considered to be the most destructive and can create large shocks. It may cause uneven drill-sting and stabilizer wear and bore-hole wall enlargement. Increasing WOB and decreasing RPM can diminish the lateral vibration.

Recognized as one of the most powerful numerical tools for solving large-scale structures of complex geometry, the finite element method (FEM) attracted many investigators in the drill-string dynamic analysis field. M.A. Trindade et al. [1] presented a study of the vibrations of a vertical slender beam. The beam was clamped on the top, pinned in the end. Its lower portion was constrained inside an outer cylinder. The beam was subject to gravity force, and geometric softening effect of its lower portion was considered in the model. The proper orthogonal decomposition method was employed in the paper to help better understand the non-linear coupled vibro-impact problem. The results of the paper showed that the micro-impacts and reaction forces at both ends are well presented only when using the non-linear axial-bending coupling model. Y.A. Khulief and H. Al-Naser [2] employed Euler-Bernoulli beam model to represent the whole elastic drill-string including both drillpipes and drillcollars (bottom hole assemble). In the report, the model was six degrees of freedom per node and accounted for the gyroscopic effect, the torsional-bending inertia coupling and gravity force effect. R. Sampaio et al. [3] employed a geometrically non-linear model to study the coupling of axial-torsional vibrations on a drill-string. The geometrical stiffening was discussed in the paper using a non-linear finite element approximation, which accounted large rotations and non-linear strain-displacements. The result of the paper showed that the responses of the linear and non-linear models after the first periods of stick-slip were considerably different. Marcelo T. Pivovan and Rubens Sampaio [4] presented a finite element model considering the coupling of axial, torsional and lateral vibrations on a drill-string. The model was subjected to distributed loads due to gravity force, impacts between the drill-string and wellbore and perturbation moments at the lower end. The results showed that the influence of the geometric non-linearities in the dynamic response of the drill-strings is crucial.

Some researchers also focus their interest on bit bounce and stick-slip vibrations in view of their great influences on drilling performance. Using a simplified lumped parameter model, Ahmet S. Yigit and Andreas P. Christoforou [5] formulated the equations of motion of a rotary drilling system. The model that adequately captures the dynamics was used in the paper to examine the interactions between the stick-slip vibrations and bit-bounce under varying operating conditions. Simulation results showed that rotational control along with axial control can effectively suppress stick-slip vibrations and bit-bounce. In their another paper [6], a fully coupled model was presented. The model accounted for bit/formation and drill-string/borehole wall interactions as well as geometric non-linearities. The results of the paper were in close agreement with field observations regarding stick-slip and axial vibrations. Y.A. Khulief et al. [7] formulated the dynamic model of drill-string using Lagrangian approach in conjunction with the finite element method. Torsional-bending inertia coupling, axial-bending geometric nonlinear coupling, gyroscopic effect are considered. Time response of drill-string system under stick-slip excitations was simulated and discussed.

It is well known that randomness exists in any real system. For drilling system, many sources of uncertainties bring randomness to the drill operation and make drill-string dynamics difficult to predict. In the late 1950s, Bogdanoff and Goldberg [8] firstly introduced the probabilistic approach to drill-string dynamics. They modeled WOB and TOB using zero-mean normally distributed process. Arnaud Chevallier [9] investigated the lateral behaviors of nonlinear drilling assemblies subject to deterministic and random excitations. The random input force was defined by its power spectral density, which was estimated on the bases of field data. T.G. Ritto et al. [10] used the non-linear Timoshenko beam theory in their paper and formulated the non-linear dynamical equations by means of the finite element method. This paper considered bit-rock interaction, fluid-structure interaction and impact forces. A random model was developed to describe the uncertainties in the bit-rock interaction. The results of the paper indicated that the uncertainties play a crucial role in the coupling among the axial, torsional and lateral responses. Partly due to the great complexity, research works on drill string dynamics from the view point of random theory are relatively rare even though the random nature has been long recognized.

The current paper presents a Euler-Bernoulli beam model of the whole elastic drill-string including both drillpipes and drill-collars. The drill-string is driven by a DC motor on the top and is subjected to distributed loads due to its own weight and constant

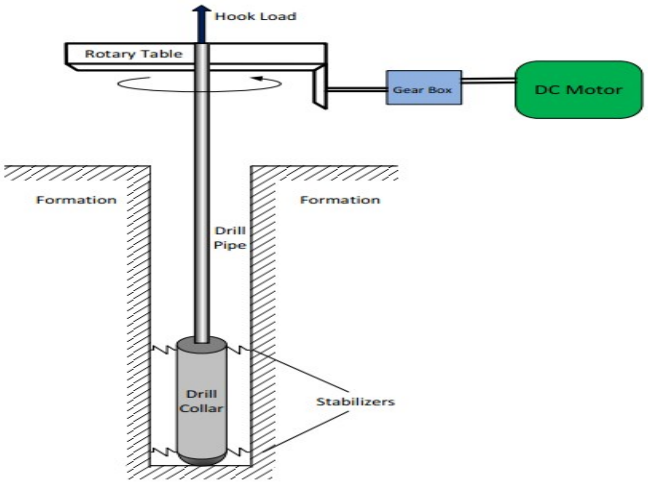

FIGURE 1. The simplified model of the system

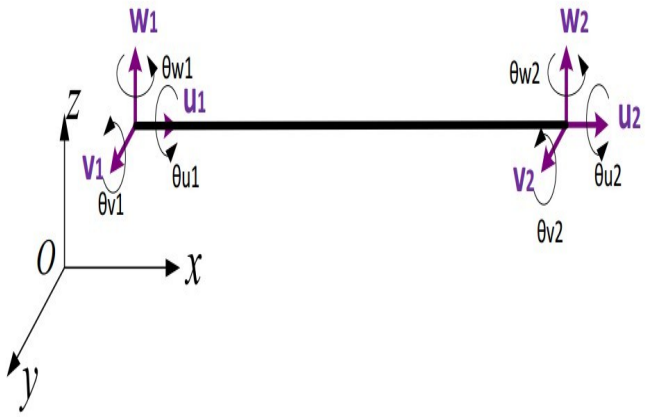

FIGURE 2. Degrees of freedom of an element

hookload. The model also accounts for bit/formation and drill-string/borehole interactions, which introduce non-linearities and randomness into the system. Rotating unbalance of the stabilizer leading to lateral vibrations is also considered. The model developed in this paper is shown in Figure 1.

DYNAMIC MODEL

Primary model

The finite element model of drill-string is discretized using Lagrange linear shape function for the axial displacement u and twisting angle θ_u and Hermite cubic functions for the lateral deflection v and w. Thus, the displacements are represented as:

$$u = N_u q,\ v = N_v q,\ w = N_w q,\ \theta_u = N_\theta q \tag{1}$$

where N_u, N_v, N_w and N_θ are shape function matrices, and q is the vector of nodal coordinates of the two-node finite element (see Figure 2), which is defined by:

$$q = \{u_1\ v_1\ w_1\ \theta_{u_1}\ \theta_{v_1}\ \theta_{w_1}\ u_2\ v_2\ w_2\ \theta_{u_2}\ \theta_{v_2}\ \theta_{w_2}\}^T \tag{2}$$

where u, v, w represent $x-$, $y-$ and $z-$ translational dofs, while θ_u, θ_v and θ_w represent the rotational dofs along the $x-$, $y-$ and $z-$ axes.

By defining the element length l_e and the non-dimensional element variable $\xi = x/l_e$, the shape function matrices are given as:

$$N_1 = 1-\xi \tag{3}$$
$$N_2 = \xi \tag{4}$$
$$N_3 = 1-3\xi^2+2\xi^3 \tag{5}$$
$$N_4 = l_e\xi(1-\xi)^2 \tag{6}$$
$$N_5 = \xi^2(3-2\xi) \tag{7}$$
$$N_6 = l_e\xi^2(\xi-1) \tag{8}$$
$$N_u = \{N_1,0,0,0,0,0,N_2,0,0,0,0,0\} \tag{9}$$
$$N_v = \{0,N_3,0,0,0,N_4,0,N_5,0,0,0,N_6\} \tag{10}$$
$$N_w = \{0,0,N_3,0,-N_4,0,0,0,N_5,0,-N_6,0\} \tag{11}$$
$$N_\theta = \{0,0,0,N_1,0,0,0,0,0,N_2,0,0\} \tag{12}$$

The expression for the linear stiffness K_e is:

$$K_e = \int_0^1 [\frac{EA}{l_e}N_u'^T N_u' + \frac{GJ}{l_e}N_\theta'^T N_\theta' + \frac{EI}{l_e^3}(N_v''^T N_v'' + N_w''^T N_w'')]d\xi \tag{13}$$

where N_u, N_θ, N_v *and* N_w are for axial, torsional and bending, respectively. The expression for the mass matrix M_e is:

$$M_e = \int_0^1 [\rho A l_e(N_u^T N_u + N_v^T N_v + N_w^T N_w) + \rho J l_e N_\theta^T N_\theta]d\xi \tag{14}$$

Substituting metrics 9 to 12 into equations 13 and 14, the linear stiffness K_e and mass M_e are obtained. The downhole damping is assumed to be a linear combination of K_e and M_e as below:

$$C = \alpha M_e + \beta K_e \tag{15}$$

where α and β are constants to be selected. In this paper the system is assumed as underdamped which is common in engineering application.

Deterministic excitations

After some mathematical manipulation, the equations of motion for the system can be represented in a compact matrix form as:

$$M\ddot{q}(t)+C\dot{q}(t)+Kq(t)=F(x,\dot{x},\phi,\dot{\phi},v,w,F_c,I) \tag{16}$$

where M, C and K are system mass, damping and stiffness matrices, respectively, $q(t)$ is the displacement vector, $F(x,\dot{x},\phi,\dot{\phi},v,w,F_c,I)$ is the excitation vector including WOB, TOB, $F_{\dot{\phi}}$, $F_{contact}$, F_{tor}, F_g, F_h and T_{rb}.
Considering the mass and stiffness of stabilizer, M and K are given as:

$$M=M_e+Am \tag{17}$$
$$K=K_e+Bk_{st} \tag{18}$$

where m and k_{st} are the mass and stiffness of the stabilizer respectively. A and B are the corresponding transformation matrices.
WOB, the weight on bit, is represented as:

$$WOB=\begin{cases} k_c(x-s)+c(\dot{x}-\dot{s}) & x\geq s \\ 0 & x<s \end{cases} \tag{19}$$

where x is the displacement of the bit, k_c is the formation contact stiffness, c is the rock damping coefficient and s is the elevation of the formation surface. k_c , c and s can be computed by [5, 12]

$$G_0=\frac{E_0}{2\times(1+\nu)} \tag{20}$$
$$k_c=\frac{G_0 r_0}{1-\nu} \tag{21}$$
$$c=\frac{3.4*r_0^2*\sqrt{G_0\rho_0}}{1-\nu} \tag{22}$$
$$s=s_0 sin(\phi) \tag{23}$$

where E_0, G_0, ν, ρ_0 are determined by the property of the rock, r_0 is the foundation diameter, ϕ is bit torsional displacement.
The torque on bit (TOB) is related with WOB and cutting conditions [5], and can be calculated by:

$$TOB=WOBr_b(\mu(\dot{\phi})+\xi_0\sqrt{\frac{\delta_c}{r_b}}) \tag{24}$$

where r_b is the radius of the bit and δ_c is the depth of cut per circle:

$$\delta_c=\frac{2\pi ROP}{w} \tag{25}$$

ROP, representing the average rate of penetration, is given as [5]:

$$ROP=c_1F_0\sqrt{w}+c_2 \tag{26}$$

where F_0 is the difference between the total weight and the hookload, w is the average bit speed. $\mu(\dot{\phi})$ is modeled as a continuous function [5]:

$$\mu(\dot{\phi})=\mu_0(tanh\ \dot{\phi}+\frac{\alpha_1\dot{\phi}}{1+\alpha_2\dot{\phi}^2}+\nu\dot{\phi}) \tag{27}$$

$F_{\dot{\phi}}$ is generated by rotating unbalance, and is given as:

$$F_{\dot{\phi}}=m\dot{\phi}^2 r \tag{28}$$

where r is the eccentric distance.
$F_{contact}$ is the contact force. Depending on if the i th node is in contact with the borehole or not, it can be calculated by:

$$F_{contact}=\begin{cases} -k_c(\sqrt{{v_i}^2+{w_i}^2}-0.05) & \sqrt{{v_i}^2+{w_i}^2}\geq 0.05 \\ 0 & \sqrt{{v_i}^2+{w_i}^2}<0.05 \end{cases} \tag{29}$$

F_{tor} is the torque given by the borehole wall when the i th node is in contact with the borehole. F_{tor} is simplified as:

$$F_{tor}=-\mu Rk_c(\sqrt{{v_i}^2+{w_i}^2}-0.05)sign(\theta_{u_i}) \tag{30}$$

where μ is a type of friction coefficient and R is the drill-collar radius. It is assumed in this paper that the stabilizer initially contacts with the borehole wall. It is also assumed that the clearance between the borehole wall and drill-collar is 0.05 m.
F_g is the elementary load vector resulting from the gravity field:

$$F_g=\int_0^1 \rho g A l_e N_u^T d\xi+Cmg \tag{31}$$

where C is the corresponding transformation matrix.
F_h is the hook load given as:

$$F_h=ratio_{constant}Weight_{drilling\ system} \tag{32}$$

In this paper, the weight of drillpipe is about 43 percent of the total weight. In order to make the drillpipe under tension and put the central point in drillcollar part, $ratio_{constant}$ is chosen to be larger than 0.5 in the simulations.
T_{rb} is the torque given by the rotary table. It is assumed in this paper that the rotary table is driven by a DC motor through a gear box and T_{rb} is given as [5]:

$$L\dot{I} + R_m I + K_m n\dot{\phi}_{rt} = V_c \tag{33}$$
$$V_c = K_m n w_d \tag{34}$$
$$T_{rb} = K_m n I \tag{35}$$

where I is the motor current and $\dot{\phi}_{rt}$ is the speed of the rotary table. w_d is assumed to be the desired table speed in this paper.

Initial deformed condition

In practice, the drill-string is lowered until the bit touches the formation. WOB_{static} grows in the event of continued lowering and finally reaches the highest static value. In addition to the WOB_{static}, the drill-string is also subjected to distributed loads due to its own weight and constant hookload at the top position. Therefore, the equation of motion for the system is written as:

$$M\ddot{q} + C\dot{q} + Kq = F_g + F_h + WOB_{static} \tag{36}$$

Notice that F_g, F_h and WOB_{static} are all time-invariant. $Ratio_{constant}$ is chosen to be 0.6. Using Matlab solver ode23t, the initial deformed condition q_0 is obtained, which will be used as the initial condition in the further simulations. From the value of q_0, it is clear that entire drillpipe and nearly 20 percent of the drillcollar is under tension. The percentage of the drillcollar can be changed by chosen different $Ratio_{constant}$. As mentioned above, in order to make the central point in drillcollar part, $ratio_{constant}$ is chosen to be larger than 0.5 in the simulations.

Model simplification

Firstly, it is assumed in this paper that stabilizer can effectively suppress lateral vibrations. Secondly, considering that the drillpipe is under tension, geometric stiffening effect will make it difficult to bend. Therefore, lateral degrees of freedom of drillpipe can be neglected. The stiffness and mass matrices for drillpipe elements are simplified as:

$$K_{pipe} = \begin{bmatrix} \frac{EA}{le} & 0 & -\frac{EA}{le} & 0 \\ 0 & \frac{GJ}{le} & 0 & -\frac{GJ}{le} \\ -\frac{EA}{le} & 0 & \frac{EA}{le} & 0 \\ 0 & -\frac{GJ}{le} & 0 & \frac{GJ}{le} \end{bmatrix} \tag{37}$$

$$M_{pipe} = \begin{bmatrix} \frac{\rho Al}{3} & 0 & \frac{\rho Al}{6} & 0 \\ 0 & \frac{\rho Jl}{3} & 0 & \frac{\rho Jl}{6} \\ \frac{\rho Al}{6} & 0 & \frac{\rho Al}{3} & 0 \\ 0 & \frac{\rho Jl}{6} & 0 & \frac{\rho Jl}{3} \end{bmatrix} \tag{38}$$

TABLE 1. Drillstring data.

Drillpipe	
Drillpipe length	$1,000\ m$
Drillpipe outer diameter	$0.127\ m$
Drillpipe inside diameter	$0.095\ m$
Drillcollar	
Drillcollar length	$200\ m$
Drillcollar outer diameter	$0.2286\ m$
Drillcollar inside diameter	$0.0762\ m$
Material	
Drillstring density	$7850\ kg/m^3$
Elastic modulus	$210\times10^9\ N/m^2$
Shear modulus	$7.6923\times10^{10}\ N/m^2$

Deterministic results

In this paper, a drillstring adopted in Ref. [11] is considered. The specification of the drillstring is listed in Table 1. The simulation results in the case when the desired table speed is 15 rad/s (142.2 rpm) and $ratio_{constant}$ is 0.6, are shown in Figure 3. It can be seen that the bit rotary speed experiences large fluctuations in this case. The rotation of the bit is slowed down to nearly zero at some points and then increased to as high as 30 rad/s (284.5rpm) at some other points. This phenomenon, as mentioned in the introduction, is known as stick-slip oscillation. A effective measure to mitigate the stick-slip in drilling operation is to increase RPM once it is detected. Figure 4 shows the simulation results when the desired table speed is increased from 15 rad/s to 30 rad/s ($ratio_{constant}$ is still 0.6). As can be

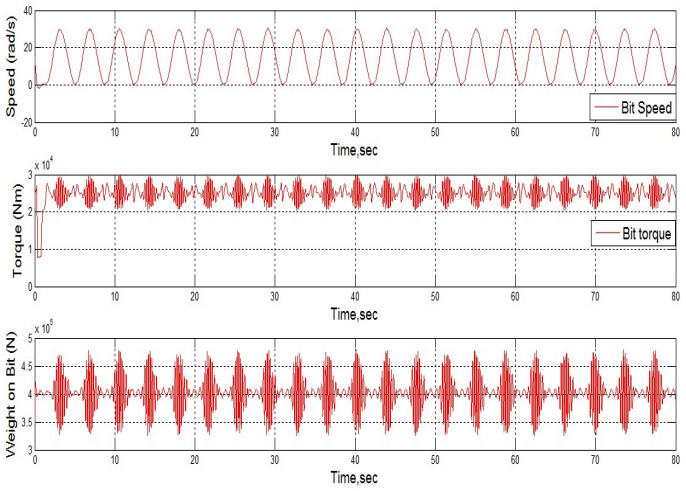

FIGURE 3. Desired table speed is 15 rad/s and stick-slip is detected

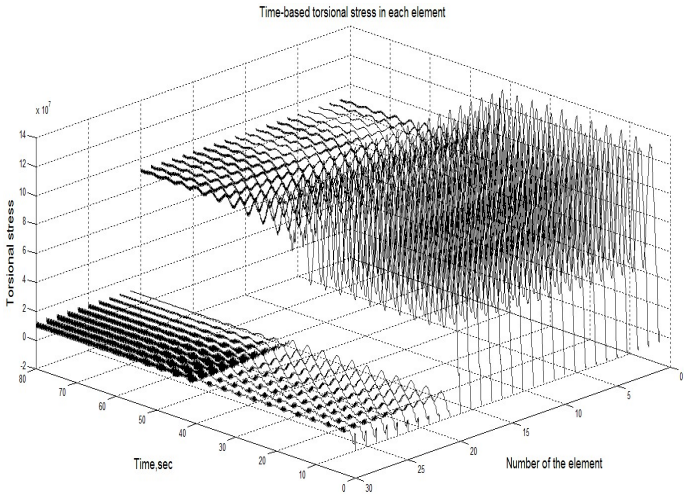

FIGURE 5. Time-based torsional surface stress of each element

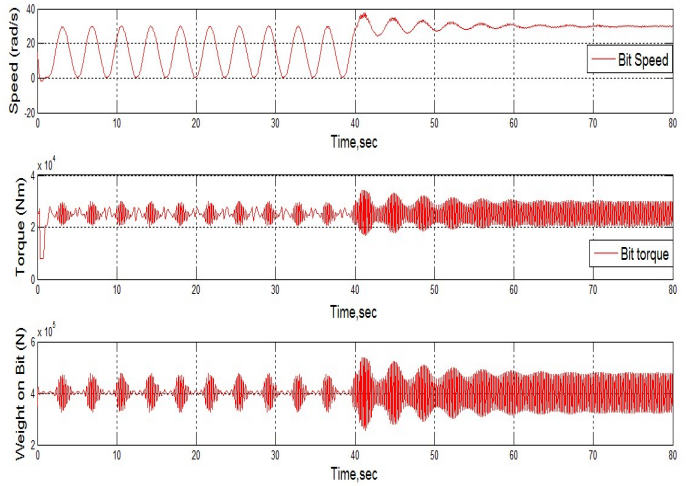

FIGURE 4. Increasing desired table speed from 15 rad/s to 30 rad/s

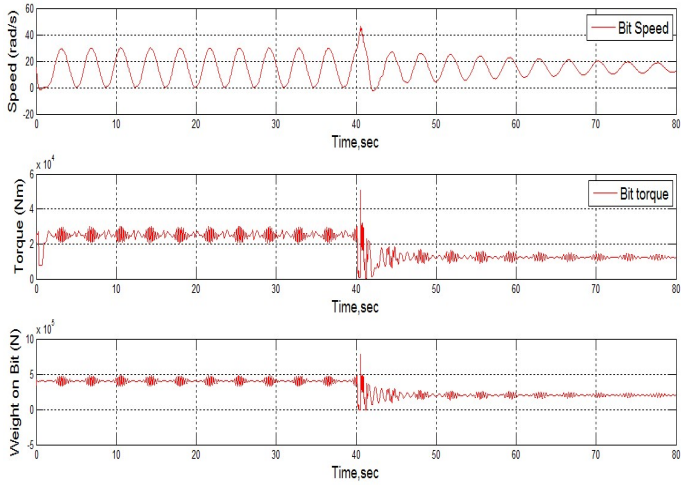

FIGURE 6. Increasing $ratio_{constant}$ from 0.6 to 0.8

seen, stick-slip is effectively eliminated at this table speed. The bit remains in contact with the formation and no bit-bounce can be found. WOB fluctuates around the static value (4×10^5 N) and the maximum amplitude remains nearly unchanged. After increasing the desired table speed from 15 rad/s to 30 rad/s, the bit rotary speed experiences large fluctuations at the beginning and then decays gradually. The reason for this may be that the torque given by the DC motor can overcome TOB and the vibrations are reduced due to damping.

Figure 5 describes the time-based torsional surface stress of each element. Element 20 is the last element of drillpipe and element 21 is the beginning element of dillcollar. Considering the cross sectional area of the later is 5.5 times larger than that of the former, the sudden change of the surface stress from element 20 to element 21 is reasonable. It can be seen that, when stick-slip happens, surface stress of the drillpipe also experiences large fluctuations. This phenomenon, if frequently happens, may enlarge surface cracks and cause premature failure of the drillpipe.

According to equation 24, WOB influences TOB; the magnitude of WOB directly affects bit torsional oscillations. Therefore, reducing WOB by increasing $ratio_{constant}$ may help relieve the problem. Figure 6 shows the simulation results when the $ratio_{constant}$ is increased from 0.6 to 0.8 and the desired table speed is kept as 15 rad/s. It can be seen that stick-slip problem is alleviated after increasing $ratio_{constant}$. However, it is also noticed that WOB is decreased by nearly 50 percent. Largely

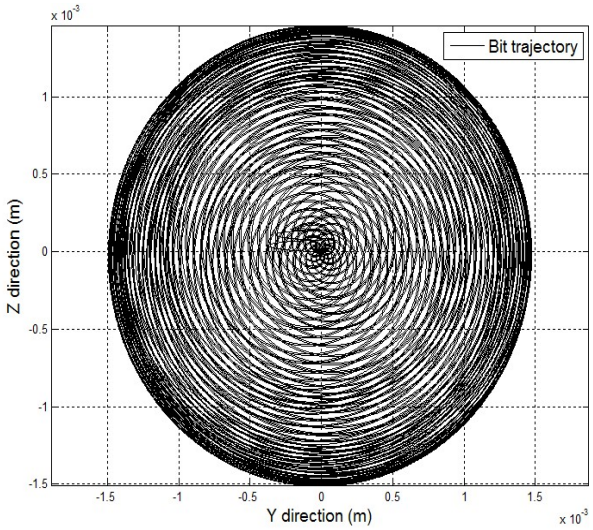

FIGURE 7. Bit trajectory when desired table speed is 15 rad/s

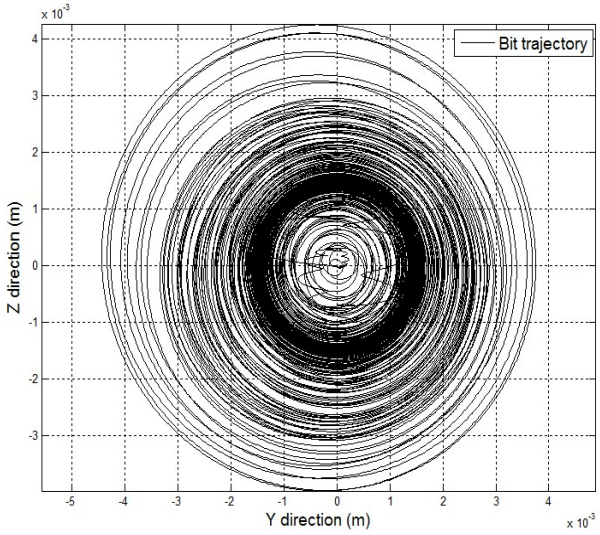

FIGURE 8. Bit trajectory when desired table speed is 30 rad/s

decreasing WOB will inevitably have negative influences on drilling efficiency, which may not be useful in the practice.

Figure 7 describes the bit trajectory when desired table speed is 15 rad/s. Rotating unbalance of the stabilizer leads to lateral vibrations, which excite bit in the lateral direction. The magnitude of the lateral vibrations depends on rotary speed, according to equation 28. When stick-slip happens, bit rotary speed periodically vibrates; therefore, bit trajectory is nearly evenly distributed in Figure 7. The denser part of Figure 8 represents the bit trajectory at the steady state when the desired table speed is 30 rad/s. As mentioned above, at the speed of 30 rad/s, large fluctuations quickly die out and the magnitude of the bit trajectory ranges from 1 to 1.5 m^{-3} due to slight vibrations. It is pretty clear that the maximum deviation of the bit in Figure 7 is about 1.5 m^{-3}. Without stick-slip, the maximum deviation should be significantly less. Therefore, stick-slip vibration not only can largely decrease ROP and cause fatigue failure of bit cutting elements, but also may lead to severe bit deviation and cause hole enlargement.

MONTE CARLO SIMULATION

Simulation procedure

According to Equations 19 to 30, the excitations of the drilling system, especially for WOB and TOB, depend on the displacement and speed vectors. The expressions of the excitations are too complex and statistical linearization is not applicable. Due to the nonlinearity of the system, spectral matrix solution method and covariance matrix solution method cannot be used directly either. Therefore, Monte Carlo simulation is employed in this paper to investigate the behaviors of drilling assemblies subject to both deterministic and stochastic excitations. In the simulation, the desired table speed is 30 rad/s and $ratio_{constant}$ is 0.6. The equation of motion for the system is given as:

$$M\ddot{q}(t)+C\dot{q}(t)+Kq(t)=F(x,\dot{x},\phi,\dot{\phi},v,w,F_c,I)+N*w(t) \quad (39)$$

where $w(t)$ is assumed to be a stationary Gaussian white noise with zero mean and spectral intensity S_0. N is a constant transformation matrix which inputs $w(t)$ to bit torsional degree of freedom.

Equation 39 is valid for any given time instant q_i. Using the central difference method, the acceleration and velocity vectors at time t_i can be written as [13]:

$$\dot{q}_i=\frac{1}{2\Delta t}(q_{i+1}-q_{i-1}) \quad (40)$$

$$\ddot{q}_i=\frac{1}{\Delta t^2}(q_{i+1}-2q_i+q_{i-1}) \quad (41)$$

Time step Δt depends on the maximum natural frequency w_n of the system. Δt is set to be 0.0002 in the paper by considering:

$$\Delta t<\frac{2\pi}{w_n}\times\frac{1}{10} \quad (42)$$

By substituting equations 40 and 41 into equation 39, and rearranging the terms one has [13]:

$$q_{i+1}=\Delta t^2 N_1 F_i+N_2 q_i+N_3 q_{i-1} \quad (43)$$

with

$$F_i = f(x, \dot{x}, \phi_i, \dot{\phi}_i, v_i, w_i, F_c, I_i) + N * w(t_i) \tag{44}$$

and

$$N_1 = [M + \frac{1}{2}\Delta t C]^{-1} \tag{45}$$

$$N_2 = N_1[2M - \Delta t^2 K] \tag{46}$$

$$N_3 = N_1[\frac{1}{2}\Delta t C - M] \tag{47}$$

M, K, C are all constant at each time step. x_i, $\dot{x}_i$, ϕ_i, $\dot{\phi}_i$, v_i, w_i and I_i are required to obtain F_i. However, equation 40 can not be used directly here to calculate $\dot{x}_i$ and $\dot{\phi}_i$. To solve this problem, velocity vectors at time t_i are calculated in the terms of:

$$\dot{q}_i = \dot{q}_{i-1} + \ddot{q}_{i-1}\Delta t \tag{48}$$

with

$$\ddot{q}_{i-1} = M^{-1}[F_{i-1} - C\dot{q}_{i-1} - Kq_{i-1}] \tag{49}$$

$f(I_i)$ is given as:

$$f(I_i) = T_{rb_i} = K_m n I_i \tag{50}$$

$$I_i = \frac{1}{L} \times (2\Delta t V_c - 2\Delta t n K_m \dot{\phi}_{i-1} - 2R_m I_{i-1}\Delta t + L I_{i-2}) \tag{51}$$

According to equation 44, the continues time white noise excitation needs to be discretized in the simulation. It is achieved by using [14]:

$$w(t_i) = \sqrt{\frac{2\pi S_0}{\Delta t}} U_i \tag{52}$$

where random variables U_i are normal distributed with zero mean and unit standard deviation.

In the simulation, U_i is generated by the computer at each step. F_i is determined at time step t_i and therefore q_{i+1} can be calculated using equation 43. For each sample, the computational procedure can be described as the following steps:

1. Initially set uniform q_0, $\dot{q}_0$, I_0 and I_{-1} for all the samples.
2. Compute $f(x_0, \dot{x}_0, \phi_0, \dot{\phi}_0, v_0, w_0, F_c, I_0)$ *and* $w(t_0)$, and then assemble F_0.

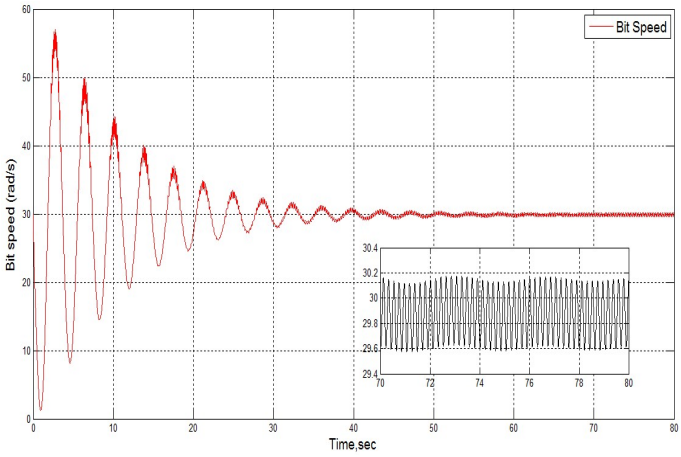

FIGURE 9. System response under deterministic excitation

3. Compute $\ddot{q}_0$ using equation $\ddot{q}_0 = M^{-1}[F_0 - C\dot{q}_0 - Kq_0]$.
4. Compute q_{-1} using equation $q_{-1} = q_0 - \Delta t\dot{q}_0 + \frac{\Delta t^2}{2}\ddot{q}_0$.
5. Start with $i = 0$.
6. Find q_{i+1} using equation 43.
7. Compute I_{i+1} using $\dot{q}_i$, I_i, I_{i-1} and equ 51, compute $f(I_{i+1})$.
8. Compute $\dot{q}_{i+1}$ using equation 48.
9. Store q_{i+1}, $\dot{q}_{i+1}$, q_i, I_{i+1} and I_i.
10. Compute $f(x_{i+1}, \dot{x}_{i+1}, \phi_{i+1}, \dot{\phi}_{i+1}, v_{i+1}, w_{i+1}, F_c, I_{i+1})$ *and* $w(t_{i+1})$, and then assemble F_{i+1}.
11. Compute $\ddot{q}_{i+1}$ using $\ddot{q}_{i+1} = M^{-1}[F_{i+1} - C\dot{q}_{i+1} - Kq_{i+1}]$.
12. $i = i + 1$.

Repeat step 6 to 12 until $i > N$. N marks the last step of the calculation. If the intensity of white noise $w(t_i)$ is set to zero, it corresponds to the deterministic case. The deterministic case can also be solved by runge-kutta method using Matlab build-in solver. Simulation results from these two methods are in excellent agreement, and are almost indistinguishable. This fact provides a verification to each method.

Response Statistics

Field test data have long recognized the random nature of down-hole vibration. However, the huge diversity and uncertainty in drilling, such as formation, resonance, dill-string well bore contact etc, make it almost impossible to determine work-for-all random intensity. In this paper, two different power spectral densities are considered simply for comparison purpose.
Figure 10 and 11 represent sample realizations of the response under deterministic excitation and a random noise with power spectral density of 200 and 2000 respectively. It can be seen that when the random intensity is low (Figure 10), the deterministic component is dominant in the response; while with increasing random intensity, the random part of the response becomes

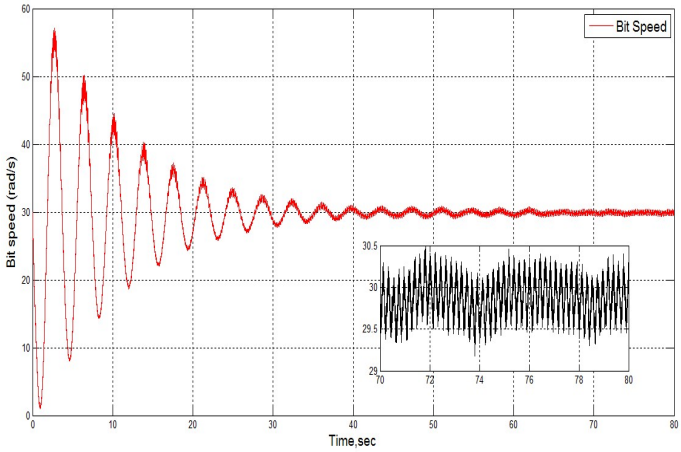

FIGURE 10. System response with white noise ($S_0 = 200$)

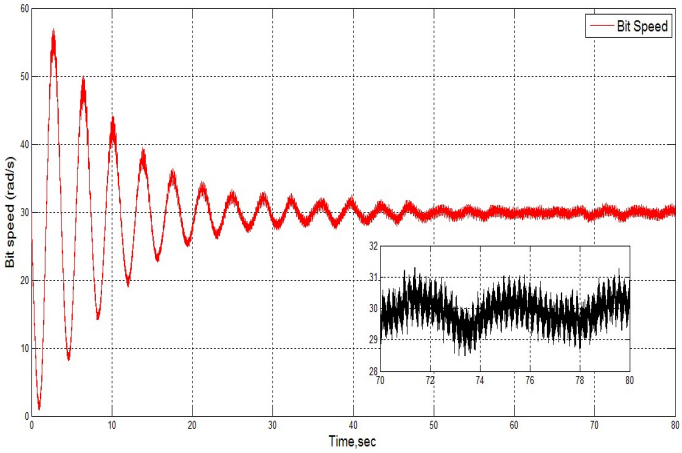

FIGURE 11. System response with white noise ($S_0 = 2000$)

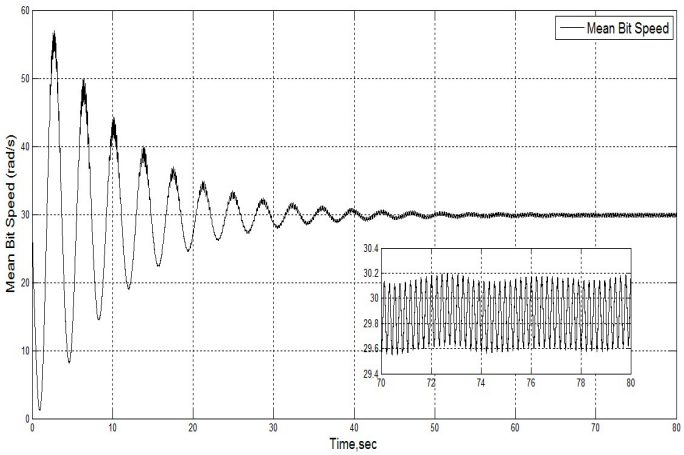

FIGURE 12. Mean bit speed (MC, $S_0 = 200$)

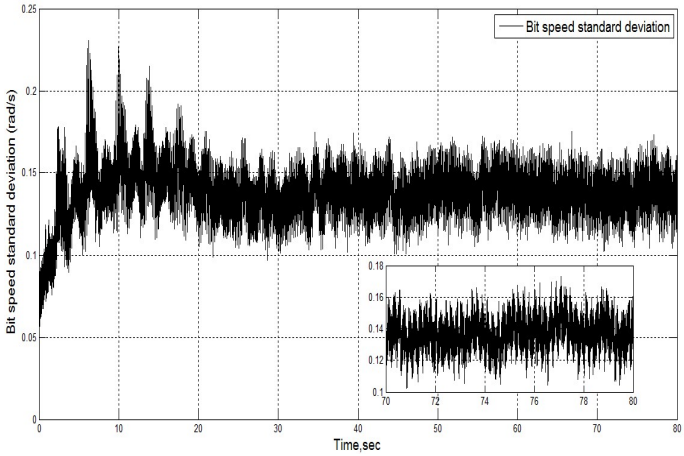

FIGURE 13. Bit speed standard deviation (MC, $S_0 = 200$)

more obvious in Figure 11. Also for comparison, the response with only deterministic excitation with desired table speed of 30 rad/s, is given in Figure 9 as well. The mean of the response with $S_0 = 200$ is given in Figure 12. It can be seen the mean is almost the same with the deterministic response in Figure 9. This is because the random excitation is assumed as zero-mean and stochastic influence ($S_0 = 200$) is limited. Figure 13 and 15 show bit speed standard deviation results with the power spectral density of 200 and 2000 respectively. The uncommon vibrations are considered due to the limited simulation samples and system's high natural frequencies. Another possible reason may be that, the axial-torsional and lateral-torsional couplings combined with changing excitations (depend on the displacement and speed vectors) lead to time variant stiffness in the model. Work for demonstrating these assumptions is underway.

Due to the many degrees of freedom and the very short time step Δt required in the simulation, the Monte Carlo simulation is very time and computer memory consuming. Precise result is difficult to obtain because of the limited 100 samples. Therefore, we pay attentions to those convincing though imprecise conclusions. As can be seen in Figure 13 and 15, the corresponding standard deviations fluctuate around 0.14 and 0.45 at the steady state. Figure 16 represents the standard deviation of bit axial displacement. Although the magnitude (10^{-4}) is small, it definitely exceeds the numerical error and therefore it is considered due to the axial-torsional coupling. The inside figure shows that the standard deviation fluctuates around $4 \times 10^{-5} m$. Figure 17 and 18 describe the standard deviations of the bit lateral displacement caused by lateral-torsional coupling. It seems that, for the drill-string model presented in the paper, torsional random exci-

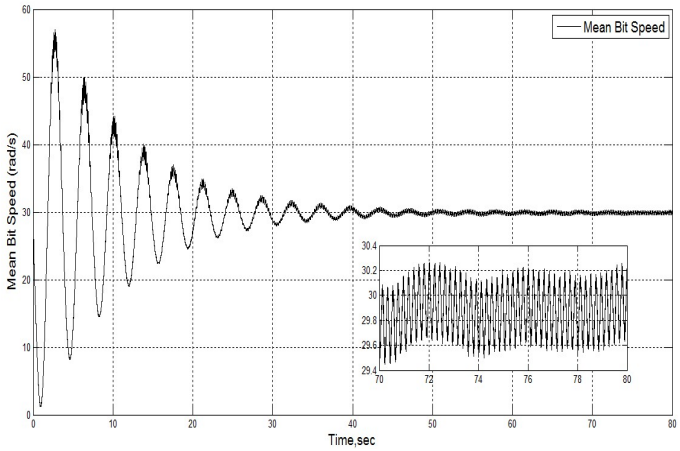

FIGURE 14. Mean bit speed (MC, $S_0 = 2000$)

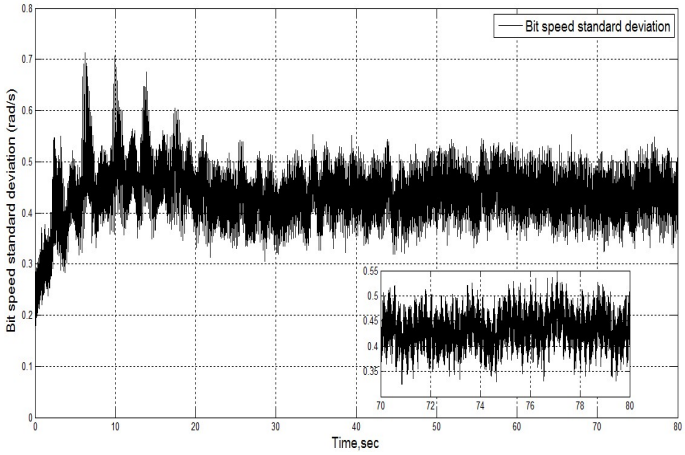

FIGURE 15. Bit speed standard deviation (MC, $S_0 = 2000$)

tation has equivalent influences in bit y and z directions. Similar result is observed when the random intensity is 2000.

CONCLUSION REMARKS

Using a finite element model with six degrees of freedom per node, this paper investigates the dynamic behaviors of a drill-string subject to both deterministic and random excitations. The model is axial-torsional, lateral-torsional coupled. MC simulation, in combination with a modified central difference method, is employed in obtaining the response statistics. The main conclusions can be drawn from this work as below:

1. Stick-slip vibration happens under certain conditions, and it can be effectively mitigated by increasing the table speed.

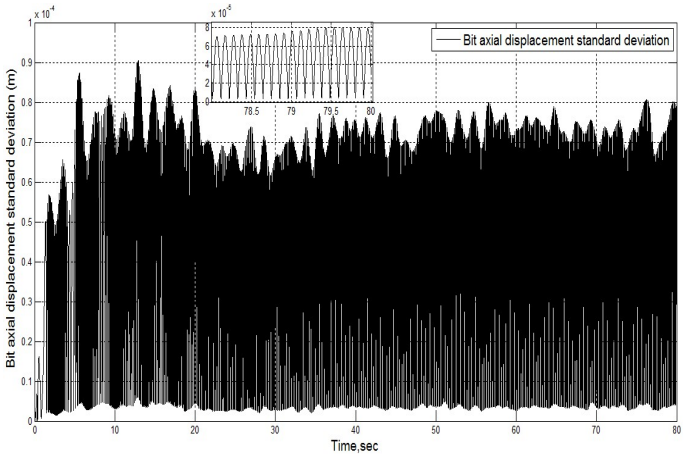

FIGURE 16. σ for bit axial displacement (MC, $S_0 = 200$)

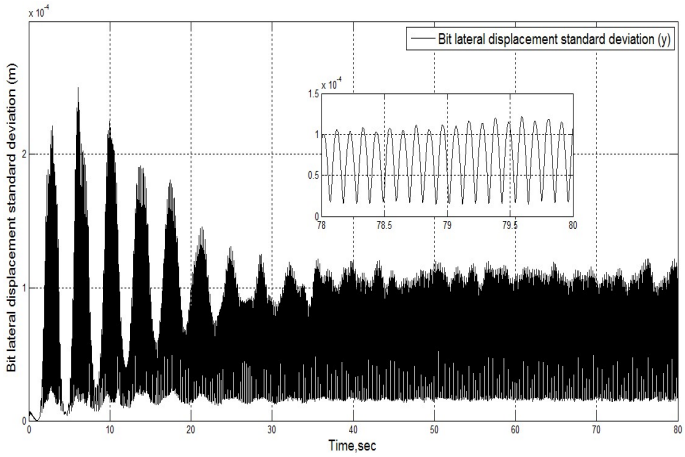

FIGURE 17. σ for bit y direction (MC, $S_0 = 200$)

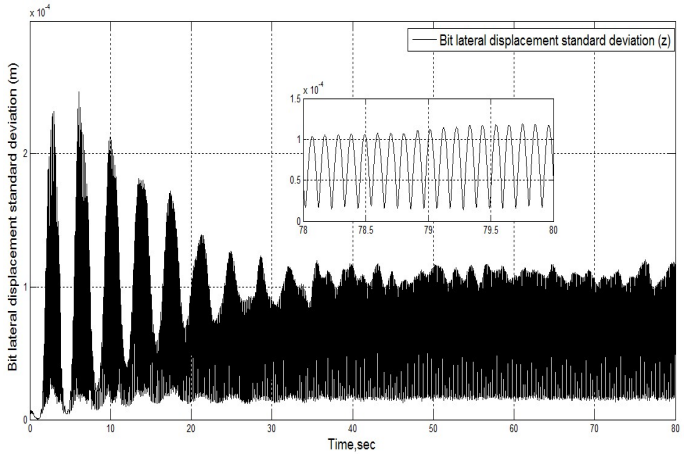

FIGURE 18. σ for bit z direction (MC, $S_0 = 200$)

2. Sometimes, rotating unbalance may lead to severe bit deviation and cause hole enlargement.
3. Axial-torsional and lateral-torsional couplings introduce random components into drill-string axial and lateral directions.

The current work does not consider the geometric stiffness and many other factors. Work in more complexed models and more effective numerical algorithm for solving the random equations is underway.

REFERENCES

[1] Trindade, M. A., Wolter, C., and Sampaio, R., 2005. "KarhunenCLove decomposition of coupled axial/bending vibrations of beams subject to impacts". *Journal of Sound and Vibration,* ***279***(3), pp. 1015–1036.

[2] Khulief, Y. A., Al-Naser, H., 2005. "Finite element dynamic analysis of drillstrings". *Finite elements in analysis and design,* ***41***(13), pp. 1270–1288.

[3] Sampaio, R., Piovan, M. T., and Venero Lozano, G., 2007. "Coupled axial/torsional vibrations of drill-strings by means of non-linear model". *Mechanics Research Communications,* ***34***(5), pp. 497–502.

[4] Piovan, M. T., Sampaio, R., 2006. "Non Linear Model for Coupled Axial/Torsional/flexural Vibrations of Drill-strings". *In III European Conference on Computational Mechanics*, January, pp. 1751–1765.

[5] Yigit, A. S., Christoforou, A. P., 2006. "Stick-slip and bit-bounce interaction in oil-well drillstrings". *Journal of Energy Resources Technology,* ***128***, pp. 268–274.

[6] Christoforou, A. P., Yigit, A. S., 2003. "Fully coupled vibrations of actively controlled drillstrings". *Journal of Sound and Vibration,* ***267***(5), pp. 1029-1045.

[7] Khulief, Y. A., Al-Sulaiman, F. A., and Bashmal, S., 2007. "Vibration analysis of drillstrings with self-excited stickC-slip oscillations". *Journal of Sound and Vibration,* ***299***(3), pp. 540-558.

[8] Bogdanoff, J. L., Goldberg, J. E., 1961. "A New Analytical Approach to Drill Pipe Breakage II". *Journal of Engineering for Industry,* ***83***, pp. 101.

[9] Chevallier, A, 2001. "Nonlinear stochastic drilling vibrations". Ph.D. Thesis, Rice University, USA. See also URL `http://hdl.handle.net`.

[10] Ritto, T. G., Soize, C., and Sampaio, R., 2009. "Nonlinear dynamics of a drill-string with uncertain model of the bitCrock interaction". *International Journal of Non-Linear Mechanics,* ***44***(8), pp. 865-876.

[11] Yigit, A. S., Christoforou, A. P., 2000. "Coupled torsional and bending vibrations of actively controlled drillstrings". *Journal of Sound and Vibration,* ***234***(1), pp. 67-83.

[12] Gazetas, G., 1983. "Analysis of machine foundation vibrations: state of the art". *International Journal of Soil Dynamics and Earthquake Engineering,* ***2***(1), pp. 2-42.

[13] To, C. W. S., Liu, M. L., 2000. "Large nonstationary random responses of shell structures with geometrical and material nonlinearities". *Finite elements in analysis and design,* ***35***(1), pp. 59-77.

[14] Bucher, C., 2009. *Computational Analysis of Randomness in Structural Mechanics*, Vol. 3 of *Structures and Infrastructures Book Series*. CRC Press. Chap. 4, pp. 112.